Charge ordering and the related structural phase transition in single-crystal $(Bi_{0.24}Ca_{0.76})MnO_3$

Y. Su, C-H. Du, and P. D. Hatton*
Department of Physics, University of Durham, Durham, DH1 3LE, United Kingdom

S. P. Collins
Daresbury Laboratory, CLRC, Warrington, WA4 4AD, United Kingdom

S-W. Cheong
Department of Physics & Astronomy, Rutgers University, New Jersey 08854
and Bell Laboratories, Lucent Technologies, Murray Hill, New Jersey 07974-0636
(Received 25 September 1998)

A single crystal of $(Bi_{0.24}Ca_{0.76})MnO_3$ has been extensively studied using both laboratory and synchrotron radiation x-ray scattering. Using x-ray techniques we can directly observe the formation of charge stripes associated with the low-temperature structural phase transition. Weak satellite peaks with a modulation wave vector $\mathbf{q}\approx(0.24, 0.24, 0)$ were observed below the transition temperature. These are associated with the charge ordering of Mn^{3+} and Mn^{4+} ions into charge (and spin) stripes within the perovskite structure. Measurements of the temperature dependence of the intensity and width of the charge-ordering satellites over the temperature range 10–240 K were also completed. These demonstrate the first-order nature of the structural phase transition that accompanies the formation of charge and spin ordering. Measurements of the width of the charge-order satellites demonstrate that the correlation length of the charge order is long range at all temperatures, and in all directions, below the structural phase transition. [S0163-1829(99)04017-5]

INTRODUCTION

Charge ordering into stripes in direct space has very recently attracted considerable attention due to its role in manganite colossal magnetoresistance[1] (CMR) and cuprate superconductivity.[2] CMR has been known to exist since 1950, but only recently has it attracted major interest.[3] This has been generated by the realization that the magnetoresistive changes can be very large and are related to the formation of spin and charge ordering.[4] Furthermore, the basic interaction responsible for the resistivity and magnetization correlation, the double-exchange interaction between neighboring Mn^{3+} and Mn^{4+} ions, is not, in itself, sufficient to explain the magnetoresistance behavior of these compounds.[5] Hole doping in the antiferromagnetic (AFM) insulators induces an insulator to ferromagnetic (FM) metal transition and for certain doping levels leads to a new type of collective state: a charge-stripe state. At these doping levels the charge ordering can compete with the FM ground state, leading to a complex electronic phase behavior as the chemical stoichiometry is varied.

Charge ordering in the maganites is generally characterized by the direct space ordering of Mn^{3+} and Mn^{4+} ions. At room temperature these ions are randomly distributed within the sample MnO_2 planes. Upon cooling the ions become regularly sited. The charge-ordered (CO) state is expected to become stable when the repulsive Coulomb interaction between the carriers (e_g electrons) dominates over the kinetic energy of carriers. The electron lattice of the CO state, therefore, acts as a Wigner crystal. Furthermore, the carriers needed to form the CO state are believed to be polarons formed from the very strong electron-phonon interaction in these materials.[6] The stability of the CO state is very sensitive to the commensurability of the hole concentration with the lattice periodicity, and hence most enhanced at nominal hole concentrations of $\frac{1}{2}$, $\frac{1}{3}$, etc.

Charge ordering has also been observed in many doped Mott-Hubbard insulators, such as $La_{2-x}Sr_xNiO_4$,[7] $La_{2-x}Sr_xMnO_4$,[8] and $La_{1-x}Sr_xFeO_3$.[9] In many cases the charge ordering is accompanied by magnetic ordering, suggesting that the interplay between charge and spin ordering is important in explaining the anomalous physical properties. Recently, a charge-ordered state with charge stripes has been observed in single crystal $La_{1.6-x}Nd_{0.4}Sr_xCuO_4$ ($x=1/8$) by neutron diffraction.[10] This has led to considerable discussion about the relationship between charge ordering and high-T_C superconductivity. Charge ordering into charge stripes is thus an important area of research applicable to a wide range of phenomenology in transition metal oxides.

To date, studies of charge ordering in these systems have generally relied upon electron diffraction and neutron scattering. Electron scattering is very sensitive to weak superlattice reflections caused by charge ordering but only in the layers near the surface. Typically, the electron diffraction studies have employed transmission geometry. This requires that the sample should be sufficiently thin to allow the electrons to traverse through the sample. Typical sample thickness is, therefore, of the order of a thousand angstroms, and samples are prepared by mechanical polishing followed by ion milling at cryogenic temperatures. Moreover, the technique has a relatively low wave-vector resolution and the measured intensities are difficult to model due to multiple-scattering effects. Neutron diffraction has been the major technique, suitable for study of both the spin and charge stripes. An unfortunate condition for neutron-scattering techniques is the need for relatively large sample sizes, which are

difficult to grow in many manganites. In addition, neutron diffraction is not directly sensitive to the charge ordering, but rather the charge order is detected indirectly through displacements of the nuclear positions because of the associated strain deforming the lattice. In this paper we report on the results of experiments on charge ordering in manganites using x-ray scattering. Our results are obtained without the use of small wavelength x-rays, which, having a greater energy penetrate almost 1 mm into the bulk employed by Vigliante *et al.*[11] in nickelate, and Zimmermann *et al.*[12] in cuprate systems. Our experiments demonstrate that it is possible to directly detect the very weak scattering from charge ordering using long wavelength x-rays, corresponding to a penetration depth of about 10 μm similar to that of the electron diffraction studies, and that x-ray scattering has an important role to play in the understanding of charge-stripe physics.

The charge stripes in the Mn^{4+} rich regime ($x>0.5$) were recently observed by electron diffraction in $La_{1-x}Ca_xMnO_3$.[13] Single crystals of this system have not yet been grown. Single crystals of the isostructural system $Bi_{1-x}Ca_xMnO_3$, however, can be grown by the flux method. Polycrystalline $Bi_{1-x}Ca_xMnO_3$ was examined for both electrical and magnetic properties, displaying ferromagnetism and a large negative magnetoresistance for $x>0.80$,[14] suggestive of charge ordering. This was recently confirmed by a neutron scattering study on single crystals for $0.74<x<0.82$.[15] That study found that the charge ordering is accompanied by a structural phase transition and that the spin fluctuations change from ferromagnetic to antiferromagnetic at the transition, with long-range antiferromagnetic order developing below T_C. The charge ordering was also observed in polycrystalline $Bi_{0.2}Ca_{0.8}MnO_3$ by electron diffraction.[16] In addition to the near 1/4 incommensurate reflections, very long period features were observed corresponding to $\frac{1}{32}$ and $\frac{1}{36}$. However, such studies cannot give quantitative intensities or provide detailed information on the long-range correlation of the static-direct space-charge stripes. More recently, phase separation behavior, in which domains of ferromagnetic and antiferromagnetic order coexist, has been reported by optical studies in $Bi_{1-x}Ca_xMnO_3$ ($x>0.5$),[17] which is consistent with a recent theoretical prediction.[18] However, the mechanism of strong interplay between charge ordering, magnetism, lattice coupling, and mesoscopic phase separation still remains unclear.

In this paper we will describe the first detailed measurements of charge-stripe formation in $Bi_{0.24}Ca_{0.76}MnO_3$ by high-resolution x-ray scattering. Using both our in-house rotating anode x-ray source and a high-resolution multiaxis diffractometer at the synchrotron radiation source (SRS) at Daresbury Laboratory, we have measured the temperature dependence of the charge-stripe satellites, which develop below the transition temperature ($T_C=241$ K). Such results indicate the strong interplay between charge stripes and the related structural phase transition.

EXPERIMENTAL PROCEDURE

The in-house x-ray experiments were performed at the University of Durham. The crystal was mounted on the cold finger of a Displex closed-cycle cryostat, where the temperature was monitored with a Si diode to an accuracy of ± 0.1 K. The whole cryostat was mounted on a four-circle triple-axis diffractometer, which employed a high-brilliance rotating anode generator operated at 2.8 kW with a Cu anode. The Cu $K\alpha$ (1.514 Å) x-ray beam was selected and collimated by two flat (0001) pyrolytic graphite crystals used as the monochromator and analyzer. Such an arrangement gives a relatively poor resolution but very high intensity.

The experiment utilizing synchrotron radiation was performed at station 16.3 at the SRS, Daresbury Laboratory. The station is situated on a beamline employing a six Tesla superconducting wavelength shifter (Wiggler 16), which provides photon beams with a wide range of energies, extending to over 50 keV. The instrument[19] is a large vertically diffracting six-circle diffractometer with a displex closed-cycle cryostat. A double-bounce Si (111) monochromator was used for the experiment, so that higher resolutions up to 10^{-4} Å^{-1} could be achieved. A wavelength of 1.000 Å was chosen to maximize the x-ray flux and a beam size of 0.5 mm horizontally and vertically was used in all measurements. Double-axis geometry using fine slits, without the use of a crystal analyzer, was employed in our measurements. Vertical beam-defining and detector slits were both set at 0.5 mm, optimized to provide good wave-vector resolution and low-background levels without sacrificing significant diffraction intensity. A cooled solid-state germanium detector was used with a narrow energy window to further decrease background scattering including fluorescence.

The single crystal of $Bi_{0.24}Ca_{0.76}MnO_3$ was grown by the flux method at Bell Laboratories. This sample had been previously characterized by a number of techniques as described in Ref. 15. In particular, the sample displays charge ordering at approximately 240 K, but does not develop AFM spin ordering until ~120 K. Most of the measurements were performed with the crystal oriented to have its [001] axis perpendicular to the scattering plane. The pseudocubic unit cell with $a=7.510$ Å, $b=7.545$ Å, $c=7.512$ Å, and $\alpha=\beta=\gamma=90°$ was used for all the measurements.

RESULTS AND DISCUSSION

This sample displayed very clean-singlet Bragg peaks with little background scatter. The experimental resolution measured at the (400) Bragg peak was 0.025 Å^{-1} in both longitudinal and transverse scans. Two-dimensional contour scans in the $(hk0)$ zone of reciprocal space were undertaken, after careful refinement of the orientation matrix. Cooling below 241 K resulted in additional satellite peaks at $(\sim\pm 0.24,\sim\pm 0.24,0)$ around the (400) Bragg peak, as shown in Fig. 1. The pseudocubic notation, with $a\approx b\approx c\approx 2a_p$ (a_p is the basic perovskite unit cell), was used in our studies, and the satellite peaks resulting from charge-ordering scattering were located along the diagonal, [110] direction in reciprocal space. However, this modulation wave vector is completely consistent with that observed by electron diffraction $(\delta,0,0)$ (Ref. 20) in the case of $La_{1-x}Ca_xMnO_3$ ($x>0.5$), which used an orthorhombic notation with $a\approx b\approx\sqrt{2}a_p$, $c\approx 2a_p$. In our diffraction pattern four satellites are found, arranged symmetrically around each Bragg peak. This is similar to the published electron-diffraction pattern[20] showing fourfold symmetry. This suggests charge ordering in the two-dimensional sheet resulting in a checkerboard pattern. How-

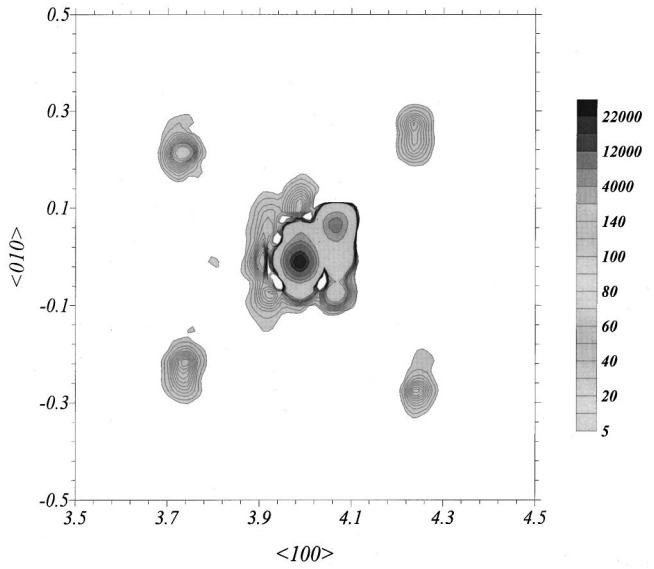

FIG. 1. Iso-intensity 2D contour map around the (400) Bragg peak in reciprocal space of $(Bi_{0.24}Ca_{0.76})MnO_3$, $T=50$ K, data obtained by using in-house rotating-anode source, 2 sec per point counting time.

ever, direct space high-resolution lattice imaging displays charge stripes running only in one direction. This apparent contradiction has been solved by complimentary dark-field images of charge charge-ordered domains in $La_{1-x}Ca_xMnO_3$.[20] These demonstrate the presence of twin-related charge-ordered domains of a few thousand angstroms in size. Discommensurations within such charge-ordered domains have also been observed, and it is likely that in our sample the diffraction pattern results from a sample that is microscopically twinned. More recently, it has been suggested that such samples may also involve an inhomogeneous spatial mixture of incommensurate charge-ordered and ferromagnetic charge-disordered microdomains, which provide a dramatic case of microscopic-scale electron-phase separation.[21]

These satellite peaks have an intensity of ~60 counts/sec, after subtracting the background of 5 counts/sec, which is almost 10^{-3} less than that of the Bragg peaks. The very weak features very close to the (400) could be sample dynamical, monochromator, and analyzer streaks because of the triple-axis configuration. Satellite peaks with a similar modulation wave vector $(\pm 0.24,\pm 0.24,0)$ were also observed around other Bragg peaks such as the (800), (620), and (6-20). Upon warming the sample above 241 K all the satellite peaks eventually disappeared, confirming the origin of these to be a superstructure of charge stripes induced by charge ordering of Mn^{3+} and Mn^{4+} in the MnO_2 sheet.

Longitudinal and transverse scans through some of the charge-ordering peaks were fitted with a Gaussian function [(Fig. 2)]. The full width at half maximum (FWHM) of the charge-ordering peaks was found to be 0.03 $Å^{-1}$, which is almost identical to that of the Bragg peaks. However, all this indicates is that the widths of both the Bragg peaks and the charge-ordered satellites are dominated by the intrinsic instrumental resolution, which is governed by the mosaic width of the graphite crystals. The charge-stripe satellites were found to be positioned at $(\pm\delta,\pm\delta,0)$ around each Bragg peak where the wave vector δ was found to be 0.24. The modulation wave vector of the charge-stripe order naturally depends upon the doped charge-carrier concentration. For a hole-carrier concentration of x, the ratio of Mn^{4+} ions to Mn^{3+} ions is $x/(1-x)$. For $x>0.5$, the modulation wave vector of the charge ordering δ is found to closely follow the stoichiometry $Bi_{1-x}Ca_xMnO_3$, according to the simple relationship $\delta=1-x$, which is identical to that reported in $La_{1-x}Ca_xMnO_3$ ($x>0.5$) by electron diffraction.[20]

The temperature dependence of the integrated intensities of the charge-stripe scattering was also measured and is shown in Fig. 3. The intensity of the CO satellites was observed to rapidly increase, upon cooling, at around 241 K (charge-ordering temperature), which occurs simultaneously with the structural phase and magnetic transition as reported in Ref. 15. No temperature dependence of the FWHM of the

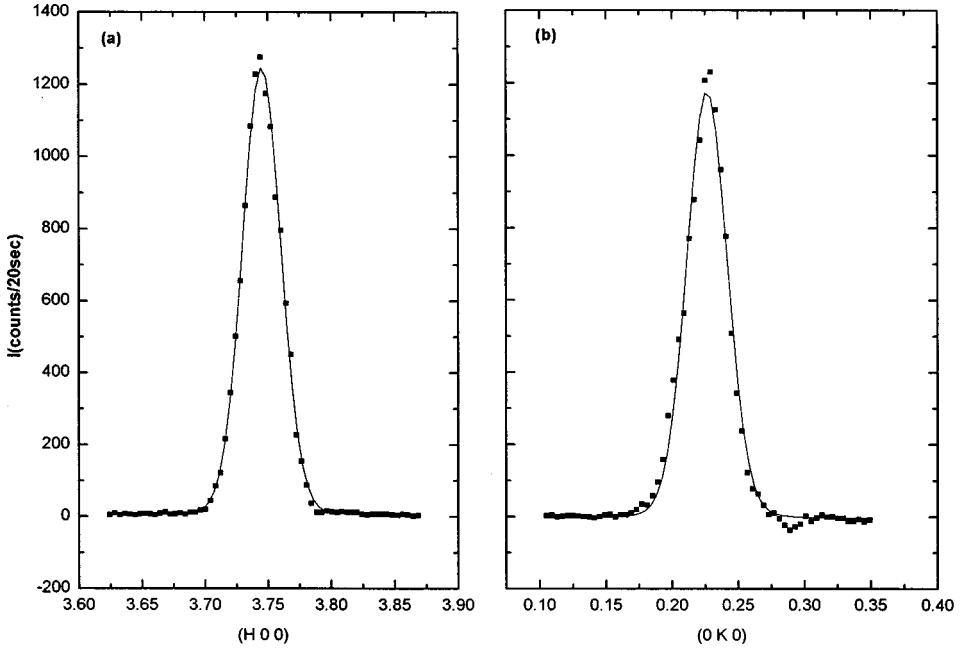

FIG. 2. (a) Longitudinal and (b) transverse scans through one of charge-stripe satellite peaks, (3.75,0.25,0) at $T=50$ K, the solid squares are the experimental data. The data can be well fitted with a Gaussian function as shown by the solid line, which gives the FWHM as 0.03 $Å^{-1}$.

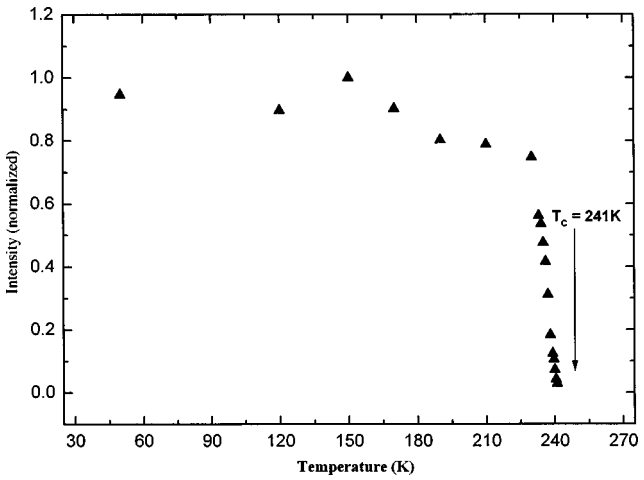

FIG. 3. The temperature dependence of the integrated intensity of the charge-stripe peak (4.25,0.25,0), which implies a transition temperature T_{CO}, of 241 K.

charge-ordering peaks was observed. Our measurements using our in-house diffractometer, fully demonstrate that it is possible to detect the relatively weak scattering from the formation of charge stripes in manganites using laboratory x-ray facilities.

Previous x-ray powder-diffraction studies by Bokov, Grigoryan, and Bryzhina[22] and neutron scattering by Bao, Axe, Chen, and Cheong[15] both indicate that the lattice parameters display a sharp discontinuity around $T_C = 241$ K, which is associated with a structural phase transition from the high-temperature orthorhombic phase to a low-temperature monoclinic phase. The coincidence of charge ordering, structural, magnetic (FM to AFM) and metal-insulator transitions implies that there is strong correlation among electronic, spin, and lattice degree of freedom. In fact, the lattice effect, or lattice distortion due to the different ionic radii of Mn^{3+} and Mn^{4+} and the tendency of Mn^{3+} to assume a Jahn-Teller distorted configuration have received considerable attention.[5,23–25] A deviation from the basic perovskite structure caused by Jahn-Teller coupling, in which some Mn-O bond lengths decrease and others increase throughout the crystal, may be determined via conventional Bragg diffraction experiments, because the changes in bond length are long-range ordered and coherent throughout crystal. Both x-ray and neutron-powder diffraction can provide the information for the average crystallographic structure and internal-structural parameters (bond distance and angle and Debye-Waller factors) and extended x-ray-absorption fine structure and neutron pair-distribution functions (PDF) can produce striking evidence for the local-lattice distortion. However, these techniques probe the structure rather than the charge stripes. X-ray scattering can simultaneously provide information on both the structure and the charge stripes.

In order to obtain both a higher resolution and a higher count rate from the charge-ordered satellites, measurements using synchrotron radiation on the same single crystal were carried out. Using the experimental configuration described above, much higher resolution was obtained (0.0054 $Å^{-1}$ FWHM) along both the longitudinal and transverse direc-

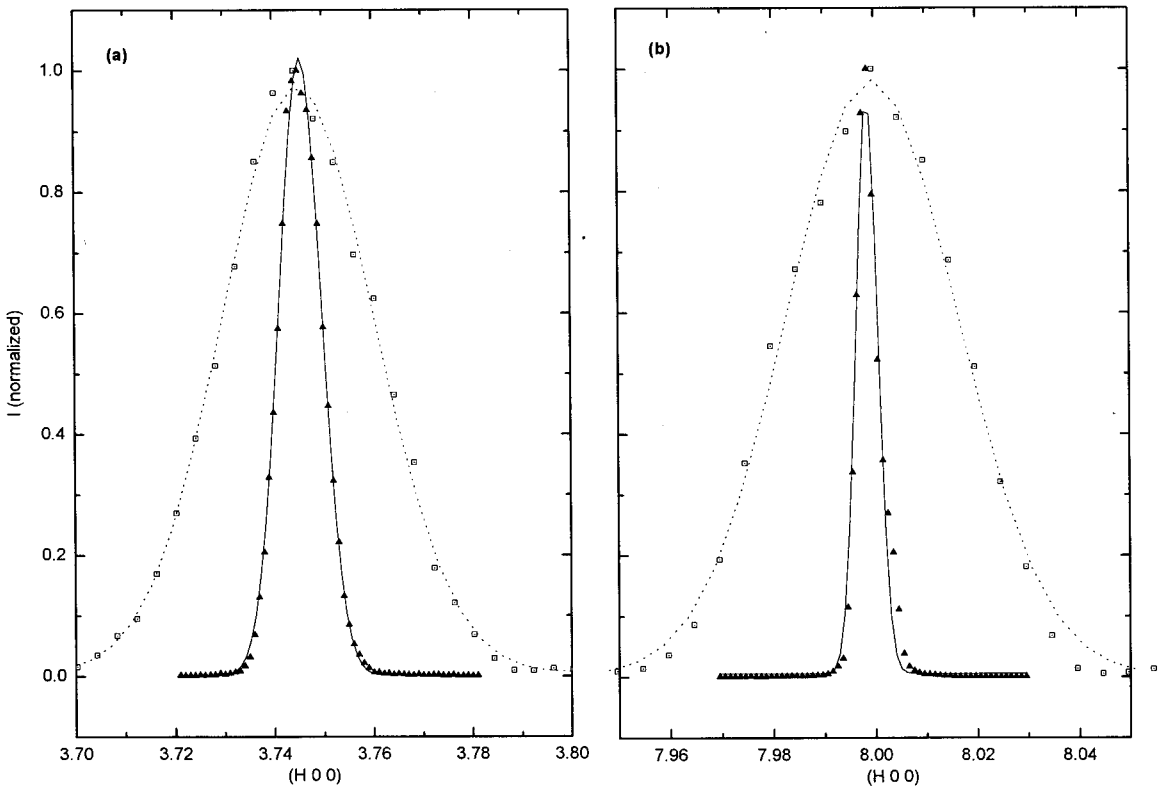

FIG. 4. (a) The charge-ordering peaks along $(H\ 0\ 0)$. (b) The $(8\ 0\ 0)$ Bragg peak along $(H\ 0\ 0)$. Both peaks are fitted by the Gaussian function, the dotted lines are fits to the laboratory low-resolution data, solid lines are fits to the synchrotron data.

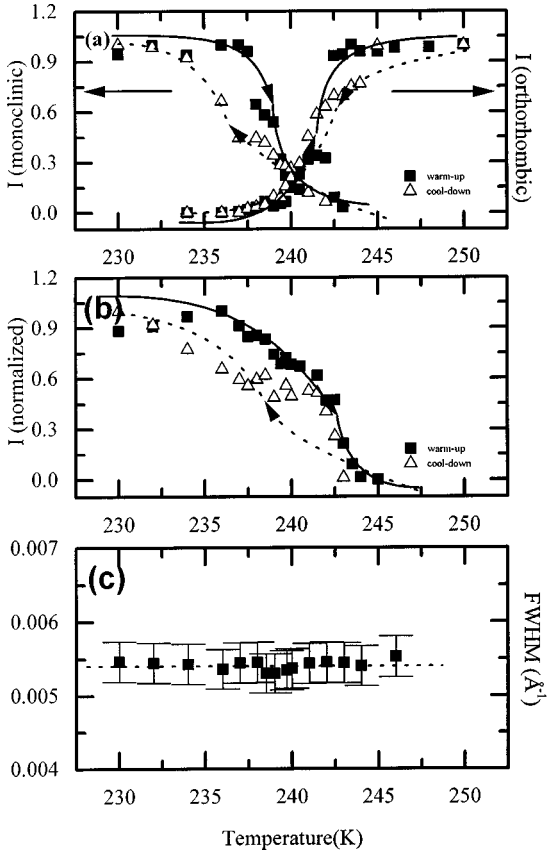

FIG. 5. (a) The integrated intensity of the (800) Bragg peak in both the high-temperature orthorhombic and low-temperature monoclinic phases. (b) The temperature dependence of the integrated intensity of the charge-stripe peak (4.25, 0.25, 0), all lines are guides for the eye. (c) The width of the charge-stripe peak, (4.25, 0.25, 0) as a function of temperature close to the structural-phase transition. The dotted line is the instrumental resolution as measured on the (400) Bragg reflection.

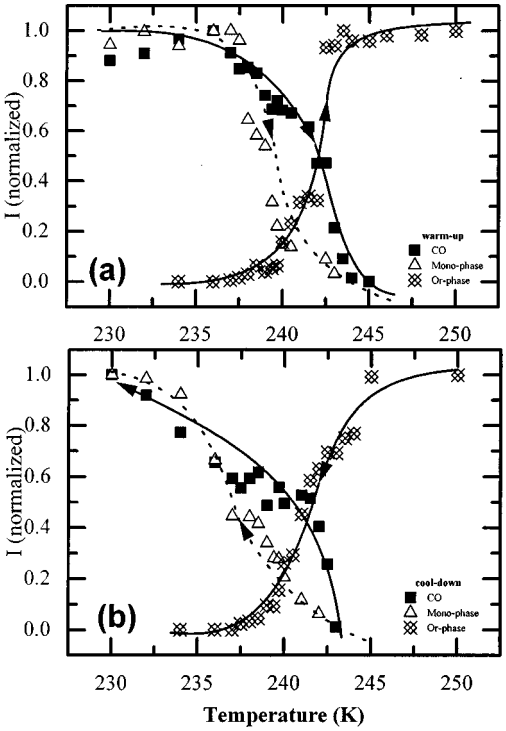

FIG. 6. (a) The integrated intensities of the charge ordering, monoclinic, and orthorhombic phase peaks upon warming up around the T_C. (b) The integrated intensities of the charge ordering, monoclinic, and orthorhombic phase peaks upon cooling down.

tions, and both the Bragg and charge-stripe peaks displayed a Gaussian peak shape (see Fig. 4). Even with the higher resolution obtainable with the use of synchrotron radiation it is clear that the quality of our sample used in this paper is not high. The rocking curve gives a full width at half maximum mosaic width of approximately $0.2°(\theta)$. This is extremely large compared to semiconductor samples (Si, GaAs, etc.) and demonstrates that extinction is not likely to affect the integrated Bragg intensities. This also explains the Gaussian peak shape and suggests that such features can be adequately treated using kinematical theory. The charge-stripe peaks were found to have an intensity as high as 10^4 counts/sec. The (800) Bragg peak in the low-temperature monoclinic phase was monitored upon warming up and through T_{CO}. At a temperature close to 240 K, the intensity abruptly dropped but did not completely disappear until 243 K. Simultaneously, the (800) peak from the orthorhombic phase, separate in reciprocal space because of the different lattice parameters between the two phases, was observed as low as 234 K, but did not become dominant until above 241 K. The sample, therefore, displays mixed-phase behavior over an extended temperature range of almost 10 K, again evidence for the first-order character of the transition. The temperature dependence of the (800) Bragg peak in the high-temperature orthorhombic phase upon cooling down is also shown in Fig. 5(a) as well. The hysteresis of the integrated intensity of the Bragg peaks is clearly demonstrated, and consistent with the first-order nature of the structural phase transition. These results place the structural phase transition boundary at 240.5 ± 0.5 K, consistent with our earlier results. The temperature dependence of charge ordering in the vicinity of T_C was also obtained via measurements of the satellite peaks along (100) and (010) in the reciprocal space. Hysteresis of the integrated intensity of the charge-stripe peaks was clearly observed as shown in Fig. 5(b). This is typical for a first-order structural phase transition.

Our results are slightly at variance with the electron-diffraction results reported by Bao on $Bi_{1-x}Ca_xMnO_3$ ($x = 0.82$),[15] where the charge-satellite intensity was observed to gradually increase upon cooling down from T_C (210 K), not becoming saturated until approximately 100 K. This may be a multiple-scattering effect rendering the intensities difficult to interpret directly. No change of the width was observed upon either warming up and cooling down as shown in Fig. 5(c). This demonstrates that the charge stripes remain long-range ordered through the transition. After careful comparison of Figs. 5(a) and 5(b), some very interesting features were noticed. Upon warming up the sample from within the low-temperature monoclinic phase, the intensity of the monoclinic Bragg peaks start to rapidly decrease at 238 K [see Fig. 6(a)]. However, the charge-stripe peaks do not display such a rapid decrease in intensity such that at 241 K (above which the high-temperature orthorhombic Bragg peaks are dominant) the intensity of the monoclinic Bragg peaks is very low, but there remains still considerable relative intensity of the charge-stripe peaks. Similarly, upon cooling down from the FM orthorhombic phase [Fig. 6(b)],

the charge-stripe intensity grows at a far more rapid pace than the development of the monoclinic Bragg reflections. These results suggest that at temperatures in the range 240–243 K there exist charge stripes, while the sample is still predominantly orthorhombic in structure.

In some related materials such as $La_{1.4-x}Nd_{0.6}Sr_xCuO_4$ (Ref. 10) and $La_{2-x}Sr_xNiO_4$,[7] the charge ordering and spin ordering occur at different temperatures. It is always found, however, that upon cooling the samples display charge ordering at a higher temperature, prior to spin ordering at yet lower temperatures. This suggests that charge ordering is the dominant driving force in the strong electron-phonon paring found in such materials. In $Bi_{1-x}Ca_xMnO_3$, only charge ordering accompanies the first-order structural phase transition. The formation of charge stripes within the orthorhombic structure will have dramatic effects on the energetics, and hence phase stability. At 240.5 ± 0.5 K the energy of the high-temperature orthorhombic and low-temperature monoclinic phases are approximately equal. Further, slow cooling results in a gradual transition from the orthorhombic to the monoclinic phase.

This also suggests that the formation of charge stripes upon cooling likely drives the structural phase transition into the low-temperature form. It is also likely that the formation of charge stripes is more continuous a transition than the clearly discontinuous structural transition. The e_g electrons hopping between the Mn^{3+} and Mn^{4+} sites results in a strong correlation between the charge, spin, and lattice, which leads to charge ordering. The charge ordering, actually a strong coupling between the charge and lattice, eventually changes the bond length of the Mn-O, until the Jahn-Teller distortions throughout the crystal reach a new equilibrium, symbolized by the formation of the long-range order and coherence of the charge and lattice. This result can be seen as a clear evidence for the strong interaction between the charge and lattice degrees of freedom.

To summarize, we have described the observation of charge ordering into stripes by x-ray scattering techniques. Such experiments can be undertaken using either synchrotron or laboratory based x-ray sources, providing new information on both structural phase transitions and the formation of charge stripes in manganites. The strong relationship between the charge-stripe ordering and the structural transition has also been discussed in detail.

ACKNOWLEDGMENTS

This paper was supported by a grant from the Engineering and Physical Sciences Research Council. We are grateful for the facilities and beamtime made available at the Daresbury Synchrotron Radiation Source. One of the authors (Y.S.) would like to thank the CVCP for support and the Department of Physics at the University of Durham for financial support during his doctoral studies.

*Author to whom correspondence should be addressed. FAX: (44) 191 374 3749; electronic address: p.d.hatton@durham.ac.uk.

[1] C. H. Chen and S.-W. Cheong, Phys. Rev. Lett. **76**, 4042 (1996); J. D. Lee and B. I. Min, Phys. Rev. B **55**, R14 713 (1997).

[2] J. M. Tranquada, J. D. Axe, N. Ichikawa, A. R. Moodenbaugh, Y. Nakamura, and S. Uchida, Phys. Rev. Lett. **78**, 338 (1997); M. I. Salkola, V. J. Emery, and S. A. Kivelson, *ibid.* **77**, 155 (1996); V. J. Emery and S. A. Kivelson, Physica C **263**, 44 (1996).

[3] A. P. Ramirez, J. Phys.: Condens. Matter **9**, 8171 (1997), and references therein.

[4] Y. Tomioka, A. Asamitsu, Y. Morimoto, H. Kuwahara, and Y. Tokura, Phys. Rev. Lett. **74**, 5108 (1995).

[5] A. J. Millis, P. B. Littlewood, and B. I. Shraiman, Phys. Rev. Lett. **74**, 5144 (1995).

[6] C. H. Chen, S.-W. Cheong, and A. S. Cooper, Phys. Rev. Lett. **71**, 2461 (1993); S. J. L. Billinge, R. G. DiFranesco, G. H. Kwei, J. J. Neumeier, and J. D. Thompson, *ibid.* **77**, 715 (1996).

[7] S.-H. Lee and S.-W. Cheong, Phys. Rev. Lett. **79**, 2514 (1997).

[8] B. J. Sternlieb, J. P. Hill, U. C. Wildgruber, G. M. Luke, B. Nachumi, Y. Morimoto, and Y. Tokura, Phys. Rev. Lett. **76**, 2169 (1996).

[9] J. Q. Li, Y. Matsui, S. K. Park, and Y. Tokura, Phys. Rev. Lett. **79**, 297 (1997).

[10] J. M. Tranquada, B. J. Sternlieb, J. D. Axe, Y. Nakamura, and S. Uchida, Nature (London) **375**, 561 (1995).

[11] A. Vigliante, M. von Zimmermann, J. R. Schneider, T. Frello, N. H. Andersen, J. Madsen, D. J. Buttrey, D. Gibbs, and J. M. Tranquada, Phys. Rev. B **56**, 8248 (1997).

[12] M. v. Zimmermann, A. Vigliante, T. Niemoller, N. Ichikawa, T. Frello, J. Madsen, P. Wochner, S. Uchida, N. H. Andersen, J. M. Tranquada, D. Gibbs, and J. R. Schneider, Europhys. Lett. **41**, 629 (1998).

[13] A. P. Ramirez, P. Schiffer, S.-W. Cheong, C. H. Chen, W. Bao, T. T. M. Palstra, P. L. Gammel, D. J. Bishop, and B. Zegarski, Phys. Rev. Lett. **76**, 3188 (1996).

[14] H. Chiba, M. Kikuchi, K. Kusaba, Y. Muraoka, and Y. Syono, Solid State Commun. **99**, 499 (1996).

[15] W. Bao, J. D. Axe, C. H. Chen, and S.-W. Cheong, Phys. Rev. Lett. **78**, 543 (1997).

[16] Y. Murakami, D. Shindo, H. Chiba, M. Kikuchi, and Y. Syono, Phys. Rev. B **55**, 15 043 (1997).

[17] H. L. Liu, S. L. Cooper, and S.-W. Cheong, Phys. Rev. Lett. **81**, 4684 (1998).

[18] S. Yunoki, J. Hu, A. L. Malvezzi, A. Moreo, N. Furukawa, and E. Dagotto, Phys. Rev. Lett. **80**, 845 (1998).

[19] S. P. Collins, R. J. Cernik, B. Fell, C. C. Tang, N. W. Harris, M. C. Miller, and G. Oszlanyi, J. Synchrotron Radiat. **5**, 1263 (1998).

[20] C. H. Chen, S.-W. Cheong, and H. Y. Hwang, J. Appl. Phys. **81**, 4326 (1997); S. Mori, C. H. Chen, and S.-W. Cheong, Nature (London) **392**, 473 (1998).

[21] S. Mori, C. H. Chen, and S.-W. Cheong, Phys. Rev. Lett. **81**, 3972 (1998).

[22] V. A. Bokov, N. A. Grigoryan, and M. F. Bryzhina, Phys. Status Solidi **20**, 745 (1967).

[23] A. J. Millis, B. I. Shraiman, and R. Mueller, Phys. Rev. Lett. **77**, 175 (1996).

[24] H. Röder, J. Zang, and A. R. Bishop, Phys. Rev. Lett. **76**, 1356 (1996).

[25] P. G. Radaelli, G. Iannone, M. Marezio, H. Y. Hwang, S.-W. Cheong, J. D. Jorgensen, and D. N. Argyriou, Phys. Rev. B **56**, 8265 (1997).